How to cite: *Angew. Chem. Int. Ed.* **2022,** *61,* e202206072
International Edition: doi.org/10.1002/anie.202206072
German Edition: doi.org/10.1002/ange.202206072

Organocatalysis Hot Paper

Transesterification of Non-Activated Esters Promoted by Small Molecules Mimicking the Active Site of Hydrolases

José J. Garrido-González, Estela Sánchez-Santos, Asmaa Habib, Ángel V. Cuevas Ferreras, Francisca Sanz, Joaquín R. Morán, and Ángel L. Fuentes de Arriba**

Dedicated to Professor Francisco Bermejo González on the occasion of his retirement.

Abstract: The synthesis of small molecules able to mimic the active site of hydrolytic enzymes has been largely pursued in recent decades. The high reaction rates and specificity shown by natural hydrolases present an attractive target, and yet the preparation of suitable small-molecule mimics remains challenging, requiring activated substrates to achieve productive outcomes. Here we present small synthetic artificial enzymes which mimic the catalytic site and the oxyanion hole of chymotrypsin and N-terminal hydrolases and are able to perform, for the first time, the transesterification of a non-activated ester such as ethyl acetate with methanol under mild and neutral reaction conditions.

Introduction

Enzymes are essential catalysts in many important industrial processes,[1] despite some drawbacks, such as its high price, sensitivity to a narrow interval of pH, temperature or ionic strength, and the restriction for most of them to work in aqueous media. In particular, hydrolytic enzymes are widely employed in the preparation of D-*p*-hydroxyphenylglycine, acrylic acid, penicillanic acid, naproxen, flurbiprofen, captopril, pantothenic acid and many other compounds for which there is no other more economical alternative.[2] Therefore, the development of stable small organic catalysts which can reproduce the high selectivity and activity of hydrolytic enzymes is both academically interesting and industrially relevant.[3]

An understanding of how enzymes are fundamentally able to catalyse reactions is essential to enable us to mimic a particular enzyme mechanism. Many hypotheses have been proposed to explain the impressive catalytic activity of enzymes,[4] perhaps the most widely accepted by Nobel Laureate Linus Pauling,[5] who suggested that the catalytic activity is caused by a larger association constant with the substrate in the transition state than in the ground state. However, it is not so clear how this large increase in the association constant is achieved by the enzyme. Whilst there are probably many different effects which act in a cooperative manner, stronger hydrogen bonds in the transition state seem to be one of the most obvious. In the case of chymotrypsin, the impressive 10^{10}-fold boost in the reaction rate can be attributed to the increase in bond strength of five of the hydrogen bonds between the enzyme active site and the reaction transition state. Two of these hydrogen bonds correspond to the oxyanion hole formed by glycine 193 and serine 195, which are responsible for a 10^4-fold increase in the reaction rate. The other three hydrogen bonds correspond to the catalytic triad, formed by a hydroxyl group from serine 195, the imidazole from histidine 57 and a carboxylate from aspartate 102, which accelerate the reaction rate by a factor of 10^6.[6] If indeed the presence of these hydrogen bonds is responsible for the rate increase, mimicking the chymotrypsin active site geometry with a simpler organic molecule should provide a similar effect on the hydrolysis rate.

More generally, other geometric factors in addition to hydrogen bonds could also influence the oxyanion stabilization. Townsend has shown that eclipsing interactions between the ground state of the amide bounded to the enzyme which are relieved upon formation of the tetrahedral intermediate could significantly affect the proteolysis reaction.[7]

Therefore, mimicking a protease active site with a relatively simple synthetic organic molecule is challenging: Cram employed a thirty-step synthesis to an artificial hydrolase by combining a cryptand receptor with a catalytic triad.[8] Other groups have also designed ingenious small organic molecules able to imitate the catalytic triad of chymotrypsin[9] however, to date, all of them are limited to the hydrolysis of activated esters such as nitrophenyl or vinyl acetates.

[*] Dr. J. J. Garrido-González, E. Sánchez-Santos, A. Habib, Á. V. Cuevas Ferreras, Dr. J. R. Morán, Dr. Á. L. Fuentes de Arriba
Organic Chemistry Department, University of Salamanca
Plaza de los Caídos s/n, 37008 Salamanca (Spain)
E-mail: josejggonzalez@usal.es
angelfuentes@usal.es
Dr. F. Sanz
X-Ray Diffraction Analysis Department, University of Salamanca
Plaza de los Caídos s/n, 37008 Salamanca (Spain)

Since N-terminal hydrolases have simplified catalytic machinery, substituting the catalytic triad for a catalytic dyad using a single N-terminal serine (or threonine) seems a reasonable approach to mimic a hydrolase enzyme. In addition, as the oxyanion hole of chymotrypsin comprises only three consecutive amino acids, is therefore simpler to mimic.

In previous work from our group,[10] the combination of a rigid aminoalcohol (acting as a catalytic dyad) with a pyridine dicarboxylic acid-based oxyanion hole led to a first hydrolase mimic **1** (Figure 1, A.1), which showed a reasonably high catalytic activity in the methanolysis of its acetate with a half-life of 3.7 min at 20 °C. **1** was also able to catalyse the transesterification of vinyl acetate with methanol at room temperature. However, comparison of **1** with the chymotrypsin active site showed that the oxyanion-hole mimic was still wider than the oxyanion hole in the enzyme. This comparison was made by superimposing the X-ray structure of compound **1**·phosphonate with the X-ray of chymotrypsin phosphate (Figure 1, A.2). Phosphonates and phosphates are good tetrahedral intermediate analogues and therefore have been used as chymotrypsin inhibitors.[11] From the X-ray structure of compound **1**·phosphonate it can be observed how the first hydrogen bond from the oxyanion hole (N–H···O = 2.89 Å) fits well with the hydrogen bond established between the NH of serine 195 and the oxygen of the phosphate in chymotrypsin (Ser N–H···O = 2.93 Å) (Figure 1, A.3). However, the second hydrogen bond in **1**·phosphonate is 0.3 Å longer than the hydrogen bonds with glycine 193 (Gly N–H···O = 2.83 Å), thus lowering the catalytic activity of the chymotrypsin mimic. In addition, the distance between the NHs of the oxyanion hole in **1**·phosphonate (4.70 Å) is longer than the average distance found in the oxyanion hole of chymotrypsin phosphate (4.27 Å) and in most natural hydrolases (4.3–4.4 Å).[12]

Trifluoromethylketones have traditionally been used as serine protease inhibitors. Their reaction with the hydroxyl group of serine 195 generates a stable hemiketal which faithfully mimics the tetrahedral intermediate of the reaction, as has been shown by recent computational analysis.[13] Furthermore, the X-ray structure of the chymotrypsin ketone inhibitor complex is available (PDB 6GCH)[14] (Figure 1, A.4) and shows even shorter hydrogen bonds between the NHs of the oxyanion hole and the tetrahedral intermediate oxygen than the phosphate inhibitor (Gly N–H···O = 2.57 Å and Ser N–H···O = 2.75 Å). However, the distance between the NHs of the oxyanion hole remains constant with the phosphate inhibitor (4.30 Å). Moreover, the neutron-diffraction structure of elastase (a chymotrypsin-like serine protease) has already been solved with a trifluoromethylketone inhibitor (PDB 3HGN)[15] and corroborates these findings: shorter hydrogen bonds between the oxyanion-hole NHs and the tetrahedral intermediate oxygen were measured (Gly N–H···O = 2.67 Å and Ser N–H···O = 2.65 Å) and the oxyanion-hole distance was established as 4.28 Å. These findings show that, in order to have a true hydrolase mimic able to compete with the catalytic activity of natural hydrolases, a shorter oxyanion

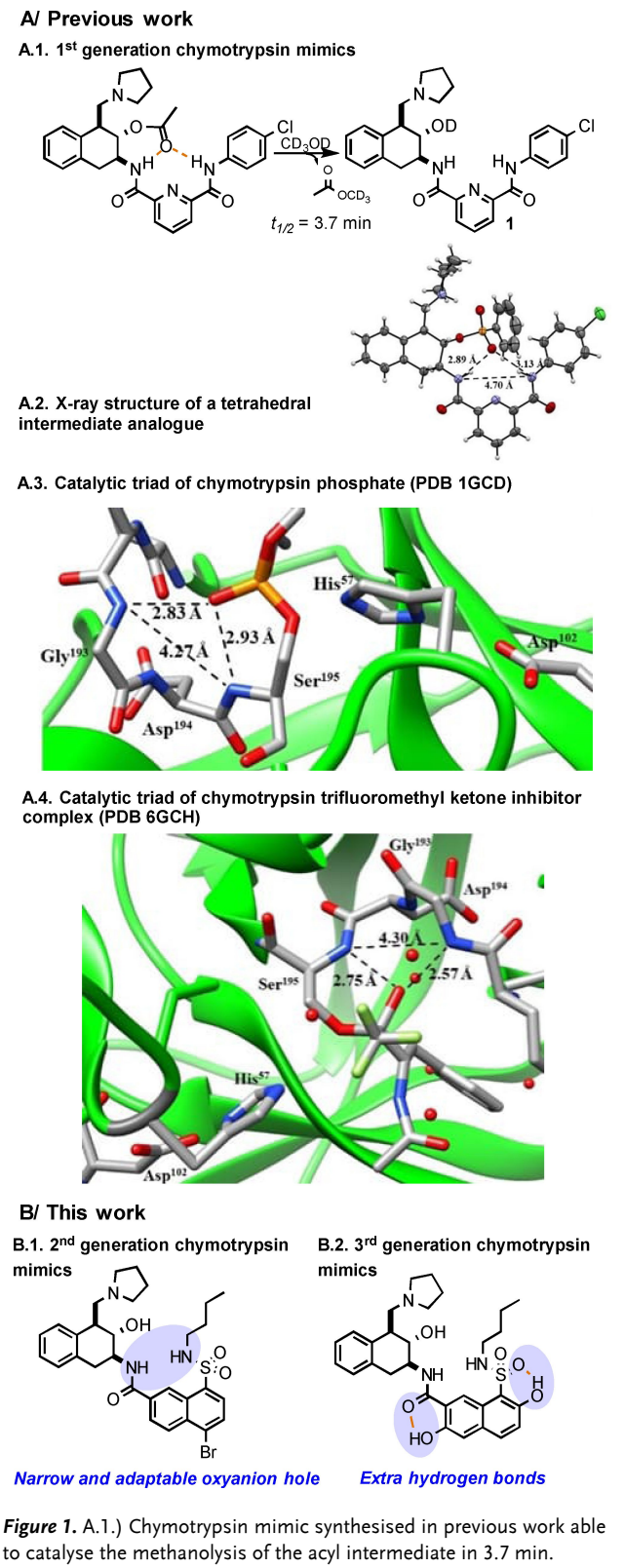

Figure 1. A.1.) Chymotrypsin mimic synthesised in previous work able to catalyse the methanolysis of the acyl intermediate in 3.7 min. A.2.) X-ray structure of a tetrahedral intermediate analogue. A.3.) X-ray structure showing the catalytic triad of chymotrypsin phosphate (PDB 1GCD). A.4.) X-ray structure showing the catalytic triad of chymotrypsin trifluoromethyl ketone inhibitor complex (PDB 6GCH). B.1.) Second generation of catalysts with a shorter and adaptable oxyanion hole. B.2.) Third generation of catalysts with extra hydrogen bonds.

hole able to form shorter hydrogen bonds with the tetrahedral intermediate is required.

We have recently reported an adaptable oxyanion-hole mimic receptor which is able to adjust the distance between both NHs according to the nature of its guest.[16] The presence of a sulfonamide at position 8 in a 2-napthoic acid skeleton confers mobility to the oxyanion-hole mimic which can then adapt to the guest to strengthen the hydrogen bonds. Building on this, the combination of this oxyanion hole with the catalytic dyad mimic aminoalcohol already optimized in our group[10] should increase the catalytic activity to a similar range to that of natural hydrolases (Figure 1B.1). In addition, the presence of a second network of hydrogen bonds with the amide carbonyl groups in the oxyanion hole should confer further stabilization to the transition state, thereby improving the catalytic performance of the hydrolase mimic (Figure 1B.2). Herein, we would like to report our findings.

Results and Discussion

Our study started with the synthesis of catalysts **3**–**6** (Figure 2, see Supporting Information for their preparation), which incorporated a naphthalene skeleton with a carboxamide in position 2 and a sulfonamide in position 8 as oxyanion-hole mimic. Different amines bearing electron donating and electron withdrawing substituents were attached to the sulfonyl group to test the influence of the sulfonamide NH acidity in the catalytic performance.

The most accepted mechanism for ester and amide hydrolysis catalysed by chymotrypsin takes place through a two-step mechanism in which an acyl intermediate is formed in the first step, followed by hydrolysis with a water molecule in the second. To test the efficiency of our hydrolase mimics in the second step, we first performed the acetylation of catalyst **3**, which was then dissolved in deuterated methanol at 20 °C and its deacetylation kinetics followed by ^{1}H NMR. Under these conditions, *pseudo*-first order reaction kinetics were proposed, and a half-life of 2.49 min was obtained (Supporting Information). This is a significant improvement on the half-life of first-generation catalyst **2** (4.8 times greater), which included an isophthalic acid oxyanion hole (Figure 2). This result shows that the new oxyanion hole based on a sulfonamide naphthalene skeleton fits better the acetate group of the acyl intermediate and sped up its methanolysis.

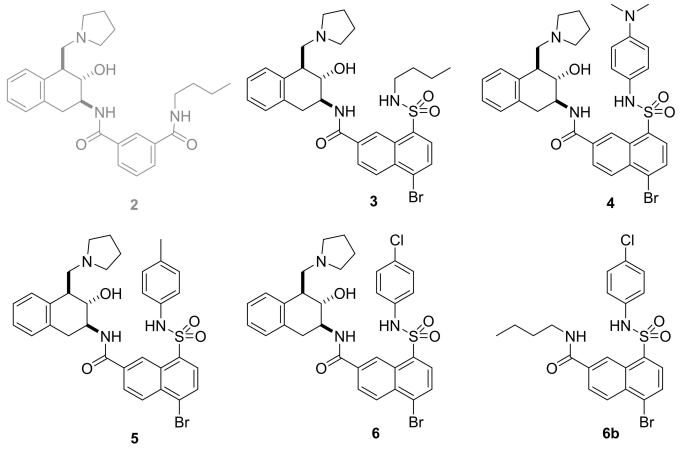

Figure 2. First- (**2**), and second-generation (**3**–**6**) hydrolase mimics and the oxyanion-hole moiety (**6b**) synthesised in this work.

Table 1 shows that the catalytic performance of compounds **4**–**6** bearing a more acidic NH in the oxyanion hole reduced the reaction time when compared with catalyst **3**. Methanolysis of acetylated catalysts **4**–**6** in pure CD_3OD was so fast that direct half-life determination by ^{1}H NMR was not possible. To reduce the reaction rate, acetylated catalysts **3a**–**6a** were dissolved in a 95/5 v/v mixture of $CDCl_3/CD_3OD$. Competitive reactions using acetylated catalyst **3a** as a reference were studied in order to have a better estimation of the speed increase when modifying the sulfonamide substituent.

The results are shown in Table 1 and show how increasing the acidity of the sulfonamide NH from 4-dimethylaniline to 4-chloroaniline boosts the reaction rate of the methanolysis reaction from 1.53 to 3.53 times *versus* catalyst **3** (Table 1, entries 2–4). This contrasts with the results obtained with first-generation catalyst **2**, which did not show any improvement when replacing the butylamide with an aromatic amide. Presumably, the NH is too far from the carbonyl oxygen of the acetate group.[10]

To confirm the importance of the oxyanion hole and the catalytic dyad being attached with the right geometry, the methanolysis reaction of **3a** was performed in the presence of equimolecular amounts of the more acidic oxyanion-hole moiety **6b** (Figure 2, Supporting Information). A half-life of 2.42 min was obtained, a result which is close to the half-life obtained for **3a** (2.49 min). This result rules out the possibility that small changes in the acidity of the media could be responsible for the rate acceleration observed.

To prove that the geometry of the oxyanion hole with the sulfonamide provided a closer NH to the acetate oxygen, the 3-nitrophenylphosphonate of catalyst **4** was prepared as a tetrahedral intermediate mimic and was crystallized (Figure 3).[17]

X-ray diffraction analysis of **4**·phosphonate showed two short hydrogen bonds of 2.85 Å and 2.77 Å between the NHs of the oxyanion hole and the oxygen of the phosphonate which mimics the negatively charged oxygen in the tetrahedral intermediate. This second hydrogen bond is

Table 1: Methanolysis reaction rate increase of acetylated catalysts (**3a**–**6a**) versus **3a**.

Entry	Catalyst	$t_{1/2}$ (**3a**–**6a**) vs. $t_{1/2}$ (**3a**)[a]
1	**3a**	1
2	**4a**	1.53
3	**5a**	2.17
4	**6a**	3.53

[a] *ca.* 10 mg of acetylated catalysts (**3a**–**6a**) were dissolved in 400 µL of $CDCl_3/CD_3OD$ 95/5. ^{1}H NMR spectra were recorded periodically at 20 °C. Half-life was determined by ^{1}H NMR integration.

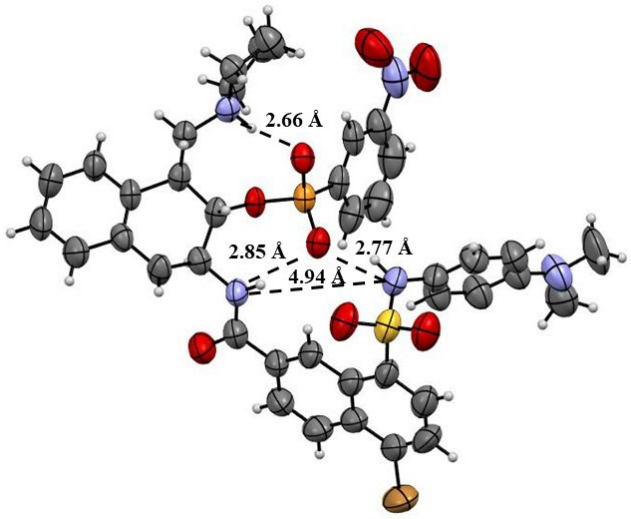

Figure 3. X-ray diffraction structure of **4**·phosphonate. Selected distances between heteroatoms are depicted in angstroms.

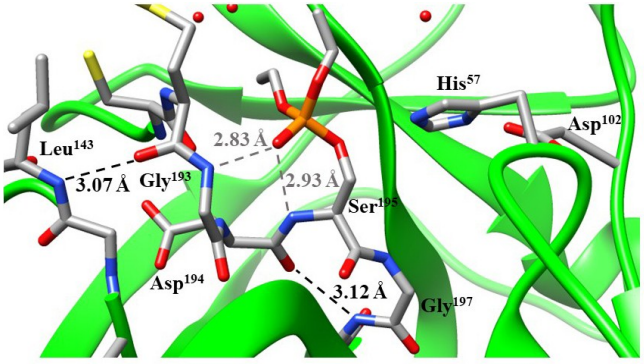

Figure 4. X-ray structure of the active centre of chymotrypsin phosphate (PDB 1GCD). Selected hydrogen bonds showing the oxyanion hole are depicted in grey and those of the second network are depicted in black.

even shorter than the hydrogen bond established with glycine 193 in the oxyanion hole of chymotrypsin (2.83 Å, Figure 1A.3). It is remarkable how the distance between the NH of the sulfonamide and the oxygen of the phosphonate is reduced by 0.36 Å in comparison with first-generation catalyst **1** (Figure 1A.2).[10] The rotation of the C–S bond gives flexibility to the sulfonamide, enabling it to adapt to the guest and reduces the hydrogen bond length between the NH and the phosphonate oxygen, making a stronger hydrogen bond.

As trifluoromethylketones make stable mimics of the transition intermediate, catalyst **3** was mixed with 1,1,1-trifluoroacetone and 2,2,2-trifluoroacetophenone. However, no hemiketal formation was observed by ^{1}H, ^{13}C, ^{19}F NMR or MS.

A striking fact in chymotrypsin catalysis is that hydrogen bonds which are placed far away from the active site have a large influence in catalysis. This is the case for the hydrogen bond of 2.83 Å between the imidazole ring of histidine 57 and the carboxylate of aspartate 102, which may contribute as much as a 10^4 factor when this hydrogen bond becomes stronger in the transition state. This may not be the only one, as many other hydrogen bonds in chymotrypsin may also increase their strength when the enzyme active site is attached to the transition state of the reaction. Analysis of the X-ray structure of chymotrypsin phosphate (PDB 1GCD) revealed the existence of two hydrogen bonds (3.07 Å and 3.12 Å) between the carbonyl groups attached to the NHs which create the oxyanion hole, and two extra NHs of the backbone (leucine 143 and glycine 197, Figure 4). This second network of hydrogen bonds could participate in fixing the conformation of the amino acids which compose the oxyanion hole in order to direct the NHs into the cavity. Alternatively, these hydrogen bonds may also reduce the transition state energy and increase the acceleration rate: they will become stronger when the negative charge is generated in the transition state and the carbonyl groups of the amides which build the oxyanion hole will also gain electron density. In fact, the significant dipole moment of an α-helix often stabilizes the oxyanion intermediate, most notably with enzymes that employ the "nucleophilic elbow" motif. The incorporation of electron withdrawing groups to the naphthalene scaffold to increase the NH acidity could mimic the electrostatic stabilization afforded by the α-helix protein scaffold.

Thus, the incorporation of a second network of hydrogen bonds into the naphthalene skeleton next to the amide and sulfonamide functionalities may be a good strategy to improve the catalytic activity of the hydrolase mimics.

To test this hypothesis, a new generation of catalysts bearing additional hydrogen bonds were synthesised. Commercially available 3-hydroxy-2-naphthoic acid allowed the synthesis of catalyst **7**, with a phenolic OH introduced in position *ortho* to the carboxamide (Figure 5). The presence of a bromine atom in C-4 was a synthetic requirement to direct the chlorosulfonation to C-8 (see Supporting Information).

Next, a competitive methanolysis reaction of acetylated catalyst **7** versus **3a** was performed in order to estimate the influence of the additional OH group in the methanolysis

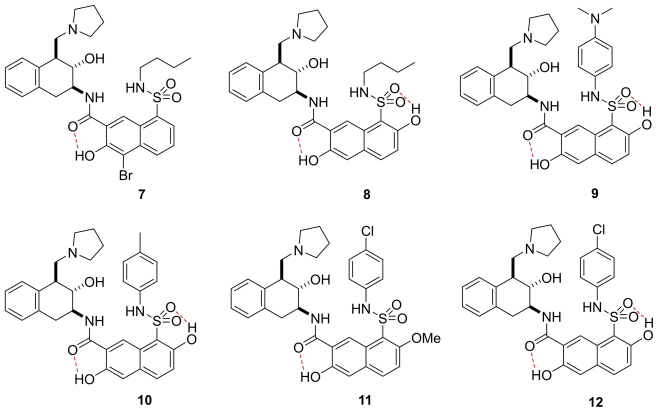

Figure 5. Third generation (**7**–**12**) of hydrolase mimics synthesised in this work with a second hydrogen bond network.

reaction rate, in this case a 4.51 fold increase in the reaction rate was observed (Table 2, entry 2). Building on this result, we targeted the synthesis of catalyst **8** from commercially available 3-hydroxy-7-methoxy-2-naphtoic acid, which incorporated a second OH in the *ortho* position to the sulfonamide. In this case, the reaction was accelerated by a factor of 8.89 (Table 2, entry 3).

To test the influence of the sulfonamide NH acidity, a series of catalysts **9**–**12** bearing both electron donating and electron withdrawing anilines was synthesised (Figure 5). After acetylation with vinyl acetate, the methanolysis reaction of each catalyst was compared with compound **3a**. Table 2 shows a correspondence between the NH acidity and the reaction rate: in general, the more acidic the sulfonamide NH, the faster the methanolysis reaction, reaching an acceleration factor of 14.97 for catalyst **12** (Table 2, entry 7). It is striking that catalyst **9** (with an aromatic sulfonamide) had a longer half-life, despite being more acidic than catalyst **8** with an aliphatic sulfonamide. The influence of the OH in the *ortho* position to the sulfonamide was obvious: catalyst **11**, in which the OH was methoxylated was only able to increase the reaction rate by a factor of 2.37 (Table 2, entry 6).

Table 2: Methanolysis reaction rate increase of acetylated catalysts (**7a**–**12a**) versus **3a**.

Entry	Catalyst	$t_{1/2}$ (**7a**–**12a**) vs. $t_{1/2}$ (**3a**)[a]
1	**3a**	1
2	**7a**	4.51
3	**8a**	8.89
4	**9a**	7.08
5	**10a**	10.44
6	**11a**	2.37
7	**12a**	14.97

[a] *ca.* 10 mg of acetylated catalysts (**3a**+**7a**–**12a**) were dissolved in 400 µL of $CDCl_3/CD_3OD$ 95/5. ^{1}H NMR spectra were recorded periodically at 20 °C. Half-life was determined by ^{1}H NMR integration.

As the half-life of catalyst **3** in neat methanol is 2.49 min, a reaction rate acceleration of 14.97 for catalyst **12** represents a half-life of 0.166 min in a 5 % $CD_3OD/CDCl_3$ solution and 0.50 seconds in neat methanol.

Acetylated catalysts were also susceptible to hydrolysis by water: compound **3a** showed a half-life of 248 min in a DMSO-d_6/D_2O 4/1 v/v solution (Supporting Information).

Figure 6 shows the methanolysis reaction rate increases of the acetylated catalysts **3a**–**12a** synthesised in this work compared with acetylated catalyst **3a** as a reference. According to Kirby's definition, the studies reported show that catalysts **3**–**12** are able to model the transacylation process catalysed by enzymes.[18]

Having optimized the catalyst oxyanion-hole moiety for the acyl intermediate methanolysis, the formation of the acyl intermediate was studied. For this first step to take place efficiently, we think that the association of the carbonyl group with the oxyanion hole is critical. First-generation catalyst **1** had already shown a low association constant for ethyl acetate (0.79 M^{-1}).[10] However, attempts to measure the association constant between catalyst **10** and ethyl acetate by ^{1}H NMR titration failed. ^{1}H NMR of catalyst **10** in $CDCl_3$ showed broad signals which did not sharpen even after the addition of three equivalents of EtOAc. A dimer may be responsible for the broad signals as the addition of AcOH, tetraethylammonium chloride (TEAC) or CD_3OD transforms the broad signals into sharp signals (Figure 7).

Nevertheless, the molar excess of acylating agent should break this dimer. In fact, while first-generation catalysts required acetic anhydride for their acetylation, second- and

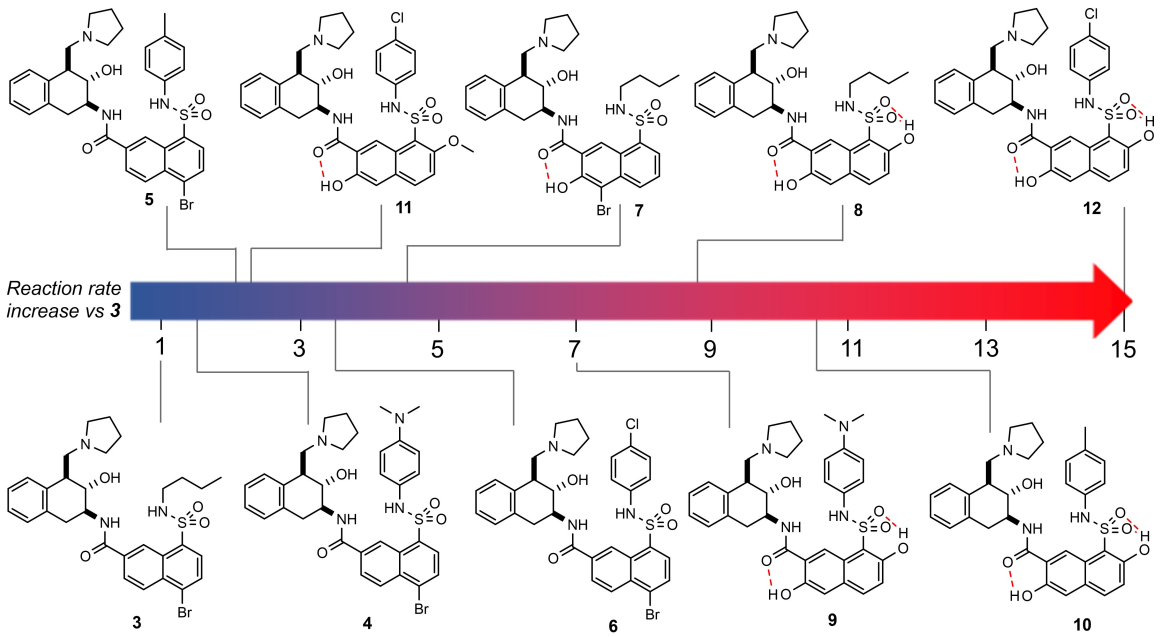

Figure 6. Methanolysis rate increase of acetylated catalysts (**3a**–**12a**) synthesised in this work.

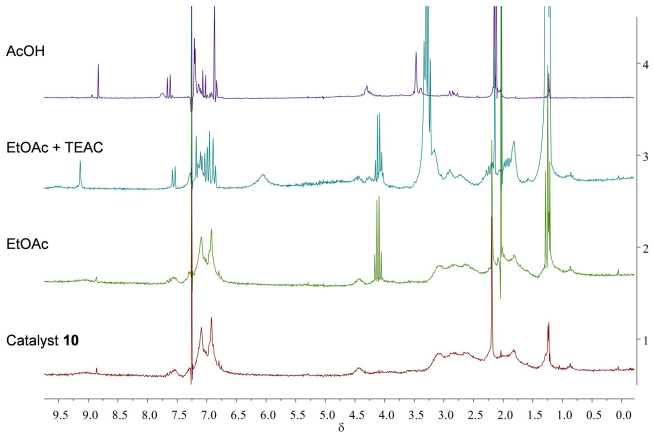

Figure 7. Catalyst **10** ^{1}H NMR spectra (9.5–0.0 ppm) before (1) and after the addition of EtOAc (2), EtOAc and TEAC (3) and AcOH (4).

third-generation catalysts were acetylated at room temperature by dissolution in vinyl acetate for a few minutes. More interestingly, second- and third-generation catalysts were susceptible to acetylation with non-activated esters such as ethyl acetate. Although the reaction was sluggish at room temperature (Table 3), it could be accelerated under reflux conditions.

Next, we investigated the hydrolysis of ethyl acetate. However, this reaction liberates acetic acid which protonates the pyrrolidine of the catalysts and inhibits further catalytic activity, requiring the addition of a basic buffer. Several auxiliary bases, such as Na_2CO_3, K_2HPO_4 and *N*,*N*-diisopropylethylamine, were tested in a biphasic solution in the presence of catalyst **3**. Ethyl acetate was replaced by the more lipophilic 2-ethylhexyl acetate in order to avoid the progress of the reaction in the aqueous phase and ensure that the catalyst (not soluble in water) was promoting the reaction in the organic phase. However, the poor solubility of water in 2-ethylhexyl acetate slowed down the reaction rate, and temperature was required to be increased to 100 °C in order to detect traces of hydrolysis product after 13 hours when Na_2CO_3 and K_2HPO_4 were used as buffers (see Supporting Information for the reaction conditions). Although THF was added to increase the solubility of water in 2-ethylhexyl acetate, after heating at 100 °C for 79.7 hours 500 mg of 2-ethylhexyl acetate with a saturated solution of Na_2CO_3 in 0.5 mL of water in the presence of catalyst **3** (0.5 mol %), a 2.8 % yield was measured by ^{1}H NMR. In the absence of catalyst, Na_2CO_3 was also able to promote the reaction with a 2 % yield.

To increase the reaction rate, homogeneous conditions were tested by dissolving catalyst **3** (2.2 mol %) in a mixture of EtOAc/Et_3N/CD_3CN/D_2O 5.6/7.8/2.8/1. The reaction mixture was heated at 50 °C in a sealed NMR tube showing a 3 % yield after 48.5 hours. Increasing the temperature to 70 °C improved the yield up to 4.5 % yield after 13 hours. No reaction was observed in the absence of catalyst.

In order to prevent the requirement for an external base and avoid the biphasic conditions which complicate the study, we next investigated the transesterification of ethyl acetate with methanol which can take place under homogeneous conditions. Catalysts **1**, **6** and **12** (0.4 mol %), as representative models of first-, second- and third-generation hydrolase mimics were dissolved in a 3:1 v/v solution of anhydrous ethyl acetate and methanol. The reactions were left at room temperature for 63 hours, and yields were measured by ^{1}H NMR integration of the crude reaction mixture (Table 4). Low conversions were obtained in all cases, however, catalyst **12** provided the best results, with a 3.6 % yield and turnover number of 8.9 after 63 hours at 23.5 °C.

Interestingly, the reaction could be accelerated by increasing the temperature to 50 °C (Figure 8). No background reaction was observed in the absence of catalyst.

To rule out that small changes in acidity of the species are responsible for the catalysis observed, the transesterification of ethyl acetate with methanol at 50 °C was studied with catalyst **3**, catalyst **3** in the presence of oxyanion-hole mimic **6b** and **6b** alone (Figure 8). Results showed that the incorporation of **6b** did not increase the transesterification rate but, on the contrary, resulted in a slight deceleration of the reaction rate probably due to competition for the

Table 3: Acetylation of catalysts **1**, **6** and **12** with ethyl acetate.

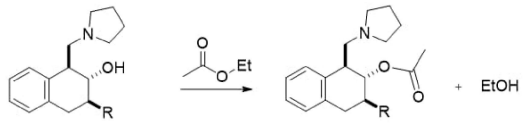

Entry	Catalyst	Yield after 24 h at rt (%)[b]	Yield after 30 min at 82°C (%)[b]
1	**1**	Traces[a]	Traces
2	**6**	30	28
3	**12**	17[a]	46

[a] The catalyst was not completely soluble in the reaction media. [b] The catalyst (0.1 mmol) was dissolved in EtOAc (0.05 M) for 24 hours. Then it was heated at 82 °C in a closed vial for 30 minutes. Yields were determined by ^{1}H NMR integration.

Table 4: Transesterification of ethyl acetate with methanol catalysed by **1**, **6** and **12**.

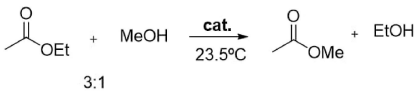

Entry¤	Catalyst¤	Yield·(%)[a]¤	TON¤
1¤	**1¤**	0.7¤	1.7¤
2¤	**6¤**	2.6¤	6.2¤
3¤	**12¤**	3.6¤	8.9¤

[a] Catalysts **1**, **6** and **12** (0.4 mol %, 0.025 M) were dissolved in a 3:1 mixture of ethyl acetate/methanol. The reaction was left at 23.5 °C for 63 hours. Yields were determined by ^{1}H NMR integration.

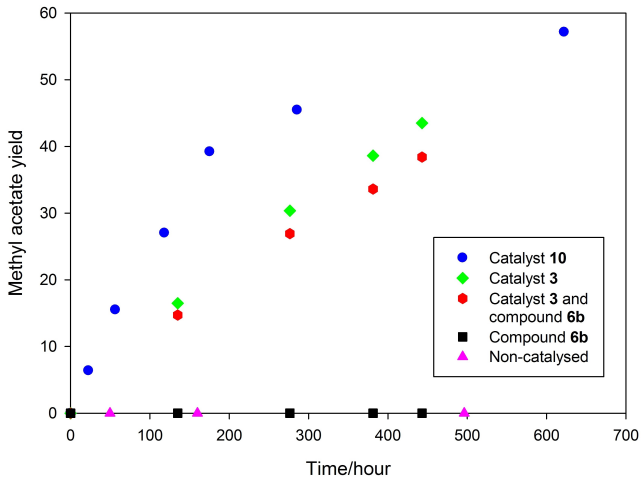

Figure 8. Transesterification of ethyl acetate with methanol (1:1.4 v/v) using catalysts **3**, **3**+**6b**, **6b** and **10** (1 mol%) at 50 °C.

hydrogen bonds of catalyst **3**. No methyl acetate was detected when **6b** was employed as catalyst. This result shows that the presence of a more acidic external oxyanion hole does not affect in the reaction and proximity between the oxyanion hole and the catalytic dyad is necessary to have an enzyme mimetic system. To the best of our knowledge this is the first time that a small molecule which mimics the hydrolase active site is able to catalyse the transesterification of a non-activated ester under mild conditions.

In addition, catalyst **3** was also able to catalyse the transesterification of acetylcholine into choline and methyl acetate.

Acetylcholine is a neurotransmitter which is involved in muscle contraction and is implicated in learning, memory, sleep, and concentration.[19]

Acetylcholinesterase converts acetylcholine into choline and acetate and its deficiency or inactivation causes cholinergic crisis, paralysis and even death.[20]

We found that catalyst **3** was able to preferentially methanolyse acetylcholine over ethyl acetate when heated in a 1:2 mixture in the presence of methanol at 50 °C in a sealed tube. After 62 hours, 71% of choline was obtained while only 7% of the ethyl acetate reacted with methanol (Figure 9).

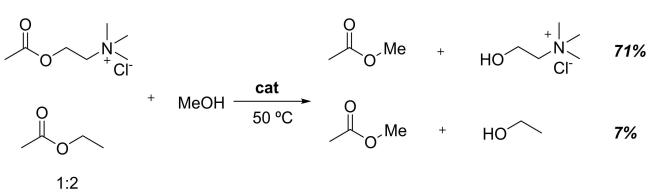

Figure 9. Competitive transesterification of acetylcholine and ethyl acetate with methanol (1:2:4.8 mol ratio) using catalyst **3** (2 mol%) at 50 °C. Yields were determined by ^{1}H NMR integration.

Conclusion

To summarise, a new family of hydrolase small mimics has been synthesised and successfully tested in the esterification reaction of non-activated esters. The oxyanion-hole moiety, constructed from a naphthalene scaffold with carboxamide and sulfonamide as hydrogen bond donors, has shown to be essential to improve the catalytic activity. An X-ray structure of the enzyme mimic covalently bonded to a phosphate (as tetrahedral intermediate mimic) showed a strong resemblance to the X-ray structure of the hydrolase active site.

Increasing the acidity of the sulfonamide, in addition to incorporating a second network of additional hydrogen bond donors, allowed the formation of the acyl intermediate with a non-activated ester as well as to increasing the rate of the methanolysis reaction to 0.50 s in neat methanol.

Remarkably, to the best of our knowledge, this is the first time that a small molecule which mimics the active centre of hydrolases is able to perform the esterification and hydrolysis of non-activated esters under mild, neutral conditions. Expanding the scope to other hydrolytic reactions will be tackled in due course.

Acknowledgements

This work was supported by MICINN (PID2020-118732RA-I00 and PID2019-108994RB-I00), Junta de Castilla y León (European Regional Development Fund-SA069P17), the University of Salamanca (Own Research Programs-KCEP/463AC01 and 18K155/463AC01) and Fundación Memoria de D. Samuel Solórzano Barruso (FS/8-2019). JJGG is gratefully acknowledged to University of Salamanca and Santander Bank for a predoctoral fellowship. AH is grateful to the Algerian Government for a predoctoral fellowship for "Formation Doctorale résidentielle à l'etranger". ALFA thanks the Spanish Government for a Beatriz Galindo Fellowship (BG20/00233). We also thank Dr. Luis Simón for preliminary molecular calculations, NUCLEUS platform at University of Salamanca, especially Anna Lithgow (NMR Service) and César Raposo and Juan F. Boyero-Benito (MS Service). Virginia Obregón from Bio-Oils Huelva is gratefully acknowledged and Dr. Victoria Atkinson for language editing.

Conflict of Interest

The authors declare no conflict of interest.

Data Availability Statement

The data that support the findings of this study are available in the Supporting Information of this article.

Keywords: Artificial Hydrolase · Enzyme Mimic · Organocatalysis · Oxyanion Hole · Transesterification

[1] K. Buchholz, V. Kasche, U. T. Bornscheuer, *Biocatalysts and Enzyme Technology*, Wiley-VCH, Weinheim, **2012**.

[2] a) H.-U. Blaser, H.-J. Federsel, *Asymmetric Catalysis on Industrial Scale*, Wiley-VCH, Weinheim, **2010**; b) K. Drauz, H. Gröger, O. May, *Enzyme Catalysis in Organic Synthesis*, Wiley-VCH, Weinheim, **2012**.

[3] a) M. D. Nothling, Z. Xiao, A. Bhaskaran, M. T. Blyth, C. Bennett, M. L. Coote, L. A. Connal, *ACS Catal.* **2019**, *9*, 168–187; b) Y. Lyu, P. Scrimin, *ACS Catal.* **2021**, *11*, 11501–11509.

[4] M. I. Page in *Enzyme Mechanisms* (Eds.: M. I. Page, A. Williams), Royal Society of Chemistry, London, **1987**.

[5] a) L. Pauling, *Nature* **1948**, *161*, 707–709; b) L. Pauling, *Chem. Eng. News* **1946**, *24*, 1375–1377.

[6] a) L. Hedstrom, *Chem. Rev.* **2002**, *102*, 4501–4523; b) R. Henderson, *J. Mol. Biol.* **1970**, *54*, 341–354; c) J. D. Robertus, J. Kraut, R. A. Alden, J. J. Birktoft, *Biochemistry* **1972**, *11*, 4293–4303; d) P. Bryan, M. W. Pantoliano, S. G. Quill, H. Y. Hsiao, T. Poulos, *Proc. Natl. Acad. Sci. USA* **1986**, *83*, 3743–3745; e) C. S. Craik, S. Roczniak, C. Largman, W. J. Rutter, *Science* **1987**, *237*, 909–913; f) S. Sprang, T. Standing, R. J. Fletterick, R. M. Stroud, J. Finer-Moore, N. H. Xuong, R. Hamlin, W. J. Rutter, C. S. Craik, *Science* **1987**, *237*, 905–909; g) P. Carter, J. A. Wells, *Proteins Struct. Funct. Genet.* **1990**, *7*, 335–342; h) D. R. Corey, C. S. Craik, *J. Am. Chem. Soc.* **1992**, *114*, 1784–1794; i) Z. Szeltner, D. Rea, T. Juhász, V. Renner, Z. Mucsi, G. Orosz, V. Fülöp, L. Polgár, *J. Biol. Chem.* **2002**, *277*, 44597–44605.

[7] A. R. Buller, C. A. Townsend, *Proc. Natl. Acad. Sci. USA* **2013**, *110*, E653–E661.

[8] D. J. Cram, *Angew. Chem. Int. Ed. Engl.* **1988**, *27*, 1009–1112; *Angew. Chem.* **1988**, *100*, 1041–1052.

[9] a) J. Lehn, C. Sirlin, *J. Chem. Soc. Chem. Commun.* **1978**, 949–951; b) D. Q. Yuan, Y. Kitagawa, K. Aoyama, T. Douke, M. Fukudome, K. Fujita, *Angew. Chem. Int. Ed.* **2007**, *46*, 5024–5027; *Angew. Chem.* **2007**, *119*, 5112–5115; c) T. Ema, D. Tanida, T. Matsukawa, T. Sakai, *Chem. Commun.* **2008**, 957–959; d) M. Kheirabadi, N. Çelebi-Ölçüm, M. F. L. Parker, Q. Zhao, G. Kiss, K. N. Houk, C. E. Schafmeister, *J. Am. Chem. Soc.* **2012**, *134*, 18345–18353.

[10] J. J. Garrido-González, M. M. Iglesias Aparicio, M. Martínez García, L. Simón, F. Sanz, J. R. Morán, Á. L. Fuentes de Arriba, *ACS Catal.* **2020**, *10*, 11162–11170.

[11] a) E. Burchacka, M. Zdzalik, J.-S. Niemczyk, K. Pustelny, G. Popowicz, B. Wladyka, A. Dubin, J. Potempa, M. Sienczyk, G. Dubin, J. Oleksyszyn, *Protein Sci.* **2014**, *23*, 179–189; b) J. Oleksyszyn, J. C. Powers, *Biochemistry* **1991**, *30*, 485–93; c) P. A. Bartlett, L. A. Lamden, *Bioorg. Chem.* **1986**, *14*, 356–377.

[12] a) L. Simón, J. M. Goodman, *J. Org. Chem.* **2010**, *75*, 1831–1840; b) L. Simón, J. M. Goodman, *Org. Biomol. Chem.* **2012**, *10*, 1905–1913.

[13] P. D. Ngo, S. O. Mansoorabadi, P. A. Frey, *J. Phys. Chem. B* **2016**, *120*, 7353–7359.

[14] K. Brady, A. Wei, D. Ringe, R. H. Abeles, *Biochemistry* **1990**, *29*, 7600–7607.

[15] T. Tamada, T. Kinoshita, K. Kurihara, M. Adachi, T. Ohhara, K. Imai, R. Kuroki, T. Tada, *J. Am. Chem. Soc.* **2009**, *131*, 11033–11040.

[16] J. J. Garrido González, I. Boya del Teso, A. L. Fuentes de Arriba, F. Sanz, E. M. Martín del Valle, J. R. Morán, V. Alcázar, *Chem. Eur. J.* **2021**, *27*, 14205–14209.

[17] Deposition Number 2144211 contains the supplementary crystallographic data for this paper. These data are provided free of charge by the joint Cambridge Crystallographic Data Centre and Fachinformationszentrum Karlsruhe Access Structures service.

[18] A. J. Kirby, F. Hollfelder, *From Enzyme Models to Model Enzymes*, RSCPublishing, Cambridge, **2009**.

[19] S. K. Fisher, S. Wonnacott, *Basic Neurochemistry: Molecular, cellular and medical aspects*, 8th ed. Elsevier, North York, **2012**, pp. 258–282.

[20] M. J. Kothari, *J. Am. Osteopath. Assoc.* **2004**, *104*, 377–384.

Manuscript received: April 26, 2022
Accepted manuscript online: May 17, 2022
Version of record online: June 7, 2022